International Endodontic Journal

doi:10.1111/j.1365-2591.2011.01930.x

Diagnostic accuracy of limited-volume cone-beam computed tomography in the detection of periapical bone loss: 360° scans versus 180° scans

S. Lennon[1], S. Patel[1,2], F. Foschi[1], R. Wilson[3], J. Davies[4], F. Mannocci[1]

[1]Department of Conservative Dentistry, Dental Institute, King's College London, London, UK; [2]Specialist Practice, London, UK; [3]Department of Periodontology, Dental Institute, King's College London, London, UK; and [4]Department of Dental Radiology, Dental Institute, King's College London, London, UK

Abstract

Lennon S, Patel S, Foschi F, Wilson R, Davies J, Mannocci F. Diagnostic accuracy of limited-volume cone-beam computed tomography in the detection of periapical bone loss: 360° scans versus 180° scans. *International Endodontic Journal*, **44**, 1118–1127, 2011.

Aim To investigate the effect of reducing limited-volume cone-beam computed tomographs arc of rotation from 360° to 180° on the ability to diagnose small, artificially created apical lesions.

Methodology Small, artificial apical bone lesions were prepared with a bur in the apical region of the distal root of ten mandibular first molars, in human dry mandibles. The jaws were scanned in a fixed position with limited-volume CBCT making a 360° and 180° arc of rotation, before and after each periapical lesion had been created. A 4 × 4 cm field of view was used at 90 kV, with a current of 4 mA. Ten examiners blinded to the scan parameters and controls scored the presence/absence of bone lesions. Intra-examiner reliability was determined after 2 weeks, reviewing half the data set. Statistical analyses with paired *t*-tests determined the diagnostic accuracy of the two modalities (360° vs. 180°) in terms of sensitivity, specificity, receiver operating characteristic area under the curve, positive predictive values and negative predictive values.

Results The mean values for sensitivity of the 360° and 180° scans were 0.91 and 0.89, respectively; their mean specificities were 0.73. No significant differences were reflected in the statistical analyses.

Conclusions Both 360° and 180° cone-beam computed tomography scans yielded similar accuracy in the detection of artificial bone lesions. The use of 180° scans might be advisable to reduce the radiation dose to the patient in line with the ICRP guidance to use as low a dosage as reasonably achievable.

Keywords: 180°, CBCT, periapical bone loss, ROC, sensitivity, specificity.

Received 4 April 2011; accepted 5 July 2011

Introduction

The question as to whether or not a periapical lesion is evident on a radiographic image is central to the discipline of endodontics. Higher success rates (9–13%) have been demonstrated in a recent systematic review (Ng *et al.* 2008a), when a periapical lesion is absent in primary root canal treatment cases. This figure rises considerably (28%) for retreatment cases (Ng *et al.* 2008b). Periapical radiographs are currently the investigation of choice with regard to the assessment of periapical status, despite many inherent limitations. A body of work in the 1960s reached the conclusion that lesions confined to the cancellous bone were not possible to detect on a periapical radiograph (Bender & Seltzer 1961a,b, Ramadan & Mitchell 1962, Wengraf 1964). Improvement in the film-distance-object standardization in the methodologies of some later studies did not alter the conclusion that the integrity of the

Correspondence: Francesco Mannocci, Department of Conservative Dentistry, King's College London, Dental Institute, Floor 25 Tower Wing, Guy's Hospital, Great Maze Pond, London SE1 9RT, UK (e-mail: francesco.mannocci@kcl.ac.uk).

cortical plate needed to be breached before changes were evident radiographically (Schwartz & Foster 1971, van der Stelt 1985).

Superimposition of anatomical structures can complicate the interpretation of a two-dimensional radiographic image. The close relationship of the maxillary sinus may present a relative radiolucency over the apices of the maxillary molar region (Huumonen & Ørstavik 2002, Patel 2009). This is because of the reduced density of the air spaces, which attenuates the X-ray beam to a lesser degree than the alveolar bone and associated dental structures (Whaites 2007). The zygomatic process may be superimposed over the region of interest and again hamper the diagnosis in this region.

A novel method of three-dimensional dental imaging has been introduced, in the form of cone-beam computed tomography (CBCT) (Arai *et al.* 1999). This provides a three-dimensional, reconstructed multiplanar imaging modality, which promises much, including the ability to overcome many of the limitations listed earlier (Patel & Horner 2009, Patel *et al.* 2009b). Essentially, there are two styles of CBCT scanners available, which differ in their volume capacity: large-volume CBCT scanners that can record the entire maxillofacial skeleton or a section of the whole dental arch and limited-volume CBCT scanners that may record small areas corresponding to 3–5 teeth depending on the region being scanned. It has been claimed that large-volume CBCT scanners produce grainier images compared with small-volume CBCT scanners not only because of increased noise from scattered radiation but also because of intrinsic limitation to avoid long reconstruction time (Scarfe & Farman 2008). It would therefore appear that limited-volume CBCT is most appropriate for endodontic diagnosis (Patel & Horner 2009).

Current CBCT machinery (both large- and small-volume devices) has the ability to image a patient by making a 360° revolution or less around the object. Clinicians are required to conform to recognized core principles on justification, optimization and limitation, as defined by the International Commission on Radiation Protection (ICRP). Sedentex CT recently released provisional guidelines regarding the application of CBCT (Horner *et al.* 2009), and a further update of these guidelines has been drafted in March 2011. Although CBCT doses are typically much lower than medical CT (Ludlow & Ivanovic 2008, Faccioli *et al.* 2009), the effective dose to the patient is higher than conventional dental planar imaging. Therefore, it is the responsibility of the clinician to maintain exposures as low as reasonably achievable. Brown *et al.* (2009) found that reducing the number of projections for 3D reconstruction did not lead to reduced dimensional accuracy and could potentially provide reduced patient radiation exposure. On some CBCT machines, a partial rotation option is available, and a recent study (Durack *et al.* 2011) demonstrated that small-volume CBCT operating with a 360° arc of rotation of the X-ray source and imaging detector is no better at detecting small, artificially created external inflammatory resorption cavities than the same device operating with 180° arc of rotation. It may be estimated that the dose reduction for the 180° scan, which reduce the exposure by half, would then reduce the effective dose by half.

Currently, there is no published data on the effect of reducing the arc of rotation by half on the detectability of small, artificial apical lesions in bone. Therefore, the aim of this study is to investigate the effect of reducing limited cone-beam computed tomographs arc of rotation from 360° to 180° on the ability to diagnose small, artificially created apical lesions in bone.

Methods

Five dry, partially dentate human mandibles were provided by the Department of Anatomy and Human Sciences (King's College, London, UK). All of the mandibles contained two-first and second molars. The jaws were rehydrated by immersion in warm soapy water (Fairy Liquid Original, Procter & Gamble, Weybridge, UK) for 90 min. The addition of the detergent allowed for increased water absorption. The rehydrated mandibles would thereby minimize the risk of root fracture during the extraction phase.

The first molar was identified in each case, and the following procedures were carried out in the same manner for each of the ten first molars under investigation in this study. The first molar was sectioned through the furcation, using a tapered 555 hi-di diamond bur (Dentsply, Addlestone, UK), in an air-rotor (Synea TA 96L-W & H; W&H, St Albans, UK). Once sectioned, the distal root was extracted intact with an upper premolar/root forceps (Hu-Friedy, Niles, IL, USA). The socket was air-dried prior to inspection under direct vision and ×12.8 times magnification, under a dental operating microscope (Global Surgical, St. Louis, MO, USA) to ensure the base of the socket was intact and had not been damaged during the extraction, before being catalogued. The root was repositioned prior to scanning.

A customized mount was fabricated to seat each of the mandibles used in the study. In brief, onto the lid of a cylindrical plastic container, medium body silicone putty (Aquasil Ultra Heavy Regular Set, Dentsply DeTrey GmbH, Konstanz, Germany) was moulded to seat each of the five mandibles. The putty was indented with each mandible to provide a stable platform.

The reference points were identified for the first mandible as follows: the contact point of the central incisors was located and traced onto the silicone putty and the plastic container. The buccal furcation of the right and left first molars was identified and traced as before. These markings created a tripod of reference points on the cylinder, which were then traced back onto each subsequent putty moulding. The mandibles were numbered 1–5. Test teeth included all first molars, a total of ten in number.

The plastic container, silicone mount and mandible were then positioned onto a wooden box on the patient seat of the Accuitomo 3D FPD (J. Morita, Kyoto, Japan) (Razavi *et al.* 2010). A hollow cylinder of acrylic (Plexiglas®, Evonik Industries, Essen, Germany) (300 mm diameter, 500 mm height and 5 mm thickness) was placed around the specimen to attenuate the beam, comparable with the presence of the soft tissues in the clinical situation (Fig. 1).

Figure 1 Overview of the experimental apparatus. (a) Accuitomo source. (b) Dry mandible mounted on the positioning device. (c) Acrylic cylinder. (d) Plastic container.

Positioning was carried out according to manufacturer's guidelines. A field of view of 4×4cm was selected, and a scout image was recorded. Subsequent minor adjustments were made, if required, so that the tooth under investigation was central in both sagittal and axial planes. The preoperative scans were then carried out at a tube voltage of 90 kV, with a current of 4mA in keeping with manufacturer's recommended exposure factors. A 4×4 cm field of view (FOV) was selected, as the most appropriate field of view to investigate a single tooth. The slice angle was reduced to −20° for mandibular right molars and increased to +20° for the mandibular left molars to align the X-ray source perpendicular to the mandibular bone. The scans were carried out at 360° and 180° at 17.5 and 9.0 s, respectively. The resultant images comprised the control data.

Preparation of artificial lesions

Artificial periapical lesions were prepared for the distal root of the first molars. The jaws were once again rehydrated as described earlier. The length of the distal root was estimated by marking the root surface at the crestal level removing the root and measuring it. The lesions were created with a 191R 160 pulp chamber bur (Meissenger, Häger & Meissenger, Neuss, Germany), with a diameter <2 mm, in a slow handpiece (WA56A; W&H). The bur was marked 1 mm longer than the corresponding root length. The bur was oriented in the long axis of the root and drilling ceased once the bur marking corresponded with the crestal level. Once the artificial lesions were created, the distal roots were repositioned and the scans were repeated, as described earlier.

The volume data were captured using iDixel 3DX (J. Morita). The data were reformatted at 0.16-mm slice intervals and 1.2-mm slice thickness. When required, the roots were also uprighted.

Radiological assessment

Ten examiners (two endodontists, two dental radiologists and six endodontic postgraduate students) were recruited to participate in the study. All examiners had considerable experience of viewing reconstructed images generated by the Accuitomo CBCT scanner. The data were presented in the Accuitomo viewing software, One Data Viewer Plus (J. Morita), and reviewed using two laptops (Hewlett Packard 2133 Netbook, Microsoft XP operating system, Acer Aspire

Timeline 5810TG -944G50Mn Laptop, Microsoft Vista operating system); each laptop was calibrated with an individual Dell screen (Dell, One Dell Way, Round Rock, TX, USA) The screens were 17'', model no. E177FPc, operating on power 100–240V, 50–60Hz, 1.5A. The screen resolution was set at 1024×768 pixels and using the highest colour quality 32 bit. Ezio software was downloaded to calibrate the corresponding screens with each laptop using RadiCS V3.22. A quiet room was used during the study period; lighting was dimmed to improve viewing conditions.

Training was carried out prior to commencing examination of the study images. The purpose of the study was explained to the examiners, and they were given an opportunity to view one of the excluded images to familiarize themselves with the software and associated tools. They were asked to examine the distal root of the first molars, using the full data set and in each case to determine whether they could detect an artificially created apical lesion.The images were randomized by entering them into a web-based application (http://www.random.org). The examiners were blinded to the scan parameters, control and test data. They were asked to score the presence/absence of a lesion using a five-point confidence scale:

- Definitely present
- Probably present
- Unsure
- Probably not present
- Definitely not present

To monitor intra-examiner reliability, all of the examiners were asked to review half the data set (a random sample of 17 images). A minimum of 2 weeks passed prior to embarking on the second viewing.

Statistical analyses were carried out using Stata™ software (Stata 10; College Station, TX, USA). The diagnostic accuracy of the two imaging modalities (360° and 180°) was analysed to determine their sensitivity, specificity, receiver operating characteristic (ROC) area under the curve, positive predictive values (PPV) and negative predictive values (NPV). The analyses were carried out using paired *t*-tests.

Table 1 Sensitivity and specificity of 360° scans compared with 180°

Examiner number	Sensitivity 360°	Sensitivity 180°	Specificity 360°	Specificity 180°
1	1.00	1.00	0.75	0.71
2	0.77	0.83	0.75	0.71
3	0.69	0.83	0.75	0.79
4	0.85	0.75	0.67	0.86
5	1.00	1.00	0.58	0.57
6	1.00	0.83	0.75	0.79
7	0.92	1.00	0.75	0.79
8	0.92	0.83	0.92	0.86
9	1.00	1.00	0.58	0.57
10	0.92	0.83	0.83	0.64
Mean (SD)	0.91 (0.11)	0.89 (0.11)	0.73 (0.10)	0.73 (0.10)
P-value	0.587		0.899	

(SD), standard deviation.
P-values derived from paired *t*-test.

Results

Sensitivity and specificity of the 360° scans compared with 180° are presented in Table 1. The mean sensitivity for the 360° and 180° scans was 0.91 and 0.89, respectively. The mean values for specificity of the 360° and 180° scans were somewhat lower at 0.73 for each. Under the experimental conditions, the examiners incorrectly diagnosed a healthy periapex 27% of the time. There was no statistically significant difference between the sensitivity or specificity of the 360° or the 180° scans. Representative images of a distal root obtained with 180° and 360° scans are presented in Fig. 2a,b, respectively.

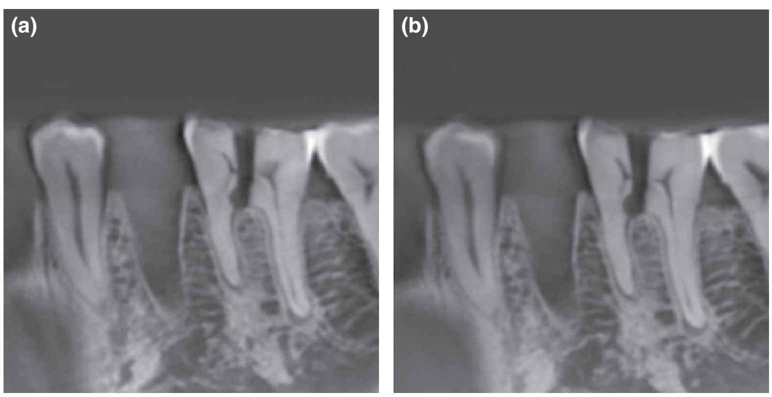

Figure 2 (a) 360° and (b) 180° arc of rotation CBCT image of the 36 showing no perceivable difference.

Table 2 Area under the curve from ROC analysis of 360° scans compared with 180°

Examiner number	ROC area under the curve (360°)	ROC area under the curve (180°)
1	0.875	0.850
2	0.734	0.856
3	0.750	0.888
4	0.805	0.888
5	0.812	0.850
6	0.922	0.913
7	0.984	0.925
8	0.953	0.981
9	0.813	0.750
10	0.875	0.819
Mean (SD)	0.852 (0.084)	0.872 (0.063)
P-value	0.429	

ROC, receiver operating characteristic; (SD), standard deviation.
P-values derived from paired *t*-test.

Further analyses included ROC area under the curves (Table 2), the mean values of which were 0.852 and 0.872 for the 360° and 180° scans, respectively. The range was from 0.734 to 0.984 for 360° and from 0.750 to 0.981 for 180° scans. There was no significant difference between the 360° and 180° scans, in terms of ROC area under the curve.

Positive and negative predictive values were analysed and are presented in Table 3. The mean PPV was 89.1 and 93.2 for 360° and 180° scans, respectively. Similarly, the NPV were 76.0 and 74.3. Again, there was no significant difference detected between the two scan parameters.

Table 3 Positive and negative predictive values for 360° scans compared with 180°

Examiner number	360° PPV	180° PPV	360° NPV	180° NPV
1	100	100	80	73
2	72	88	67	70
3	60	89	67	78
4	83	90	70	88
5	100	100	67	62
6	100	89	80	78
7	100	100	80	80
8	88	90	88	88
9	100	100	73	62
10	88	86	88	64
Mean (SD)	89.1 (14.0)	93.2 (6.0)	76.0 (8.3)	74.3 (9.8)
P-value	0.272		0.653	

PPV, positive predictive values; NPV, negative predictive values; (SD), standard deviation.
P-values derived from paired *t*-test.

Kappa scores were used to assess the interexaminer reliability. The mean values were found to be 0.858 and 0.64 for 360° and 180° scans. The scores ranged between 0.26 and 1.00 for the 360° scans and between 0.33 and 1.00 for the 180° scans, respectively. No significant difference was detected between the two scan parameters.

Further, Kappa analyses were applied to determine the intra-examiner reliability, and the mean of which was found to be 0.232 and 0.32 for the 360° and 180° scans, respectively.

Discussion

In endodontics, diagnosis is reached by making a judgement based on the patient history and clinical signs and symptoms of pulp and/or periapical disease (Pitt Ford & Patel 2004). It is understood however that the correlation between these signs or symptoms with the actual histological findings is poor (Seltzer *et al.* 1963, Dummer *et al.* 1980). Similarly, the planar radiographic representation of apical periodontitis is frequently underestimated when compared with histological examination, which is regarded as the 'reference standard'. It was not the intention of this study to compare the diagnostic accuracy of CBCT with that of planar radiography, as there is already an abundance of research published in this area. Current available evidence suggests that CBCT may detect periapical rarefaction more frequently and at an earlier stage of development than conventional radiographic methods (Lofthag-Hansen *et al.* 2007, Estrela *et al.* 2008, Jorge *et al.* 2008, Garcia de Paula-Silva *et al.* 2009, de Paula-Silva *et al.* 2009).

The diagnostic accuracy of a test can be described in terms of its percentage correct, sensitivity, specificity or area under the ROC curve. Percentage correct is of limited value as a test measure, as it will vary according to the prevalence of the disease (Metz 2006) and was therefore not assessed for the purpose of this study. Radiographic examination is an integral tool used in endodontic diagnosis. It is a required component of the preoperative assessment, subsequent post-treatment review and follow-up (ESE 2006). The validity of a diagnostic test to accurately inform the presence of a disease may be expressed in statistical terms as its sensitivity and specificity.

The findings of this study reveal a mean sensitivity of 0.91 (360°) and 0.89 (180°), which compares favourably with de Paula-Silva *et al.* (2009), who demonstrated a sensitivity of 0.91 in a dog study, which was confirmed with histological assessment. Stavropoulos & Wenzel (2007) recorded sensitivity of 0.54, in their *ex vivo* study using pig jaws. When compared with planar imaging, Patel *et al.* (2009a) concluded that the sensitivity of limited cone-beam computed tomography was found to be significantly better than that of periapical radiography. This study compared periapical radiography with limited-volume cone-beam computed tomography in the detection of small and large artificially created apical lesions in human mandibles. The overall sensitivity and specificity for periapical radiography were 0.25 and 1.0, respectively, whereas limited-volume CBCT revealed both values as 1.0. The mean values for specificity were 0.73 for both the 360° and 180° scans, in the present study, were found to be comparable (0.75) with the findings by Stavropoulos & Wenzel (2007).

In this instance, sensitivity for both the 360° and the 180° scans approached 1.0, which is a positive reinforcement of the diagnostic accuracy of both imaging methods. However, the results also present a paradox: Why is it that an imaging technique that appears to be highly sensitive returns specificity values (0.73) which could be regarded as less than moderate (Obuchowski 2003)? A healthy periapex was diagnosed correctly in only 73% of cases. The implication of the incorrect diagnosis of a disease state could lead to the provision of inappropriate or unnecessary treatment.

It is recognized that the readers' decision threshold will also influence the sensitivity and specificity of a diagnostic test (Metz 2006). This could reflect the reader skill or their decision process, which is influenced by how aggressively they detect an abnormality. Perhaps, it reflects the limitation of an *ex vivo* study model, where the patients' prior medical history is unavailable. Osteopenic patients often display sparse trabecular pattern in the mandible (Jonasson *et al.* 2009). Some of the specimens presented with sparse trabeculation (which acts as anatomical noise) further complicating the detection of small radiolucencies. In the clinical setting, radiographic findings are supported by the patient history and additional special tests (Metz 1978). The artificial lesions created for the purpose of this study were intentionally small and limited to cancellous bone. Stavropoulos & Wenzel (2007) examined detectability of artificially created lesions of three different sizes and as a result excluded lesions greater than the 3 × 3 mm, because of the fact that they were readily detectible on periapical radiographs. The present study selected small lesions, as the usefulness of CBCT in detecting small lesions, which may otherwise be missed by planar imaging (Patel & Horner 2009) was being investigated. The presentation of artificial lesions is unlike that of a naturally occurring lesion associated with chronic apical periodontitis. Goldman noted that chronic lesions characteristically demonstrated a sclerotic border (Goldman *et al.* 1972). The 'halo' effect of naturally occurring lesions was described by Pitt Ford (1984), where the loss of lamina dura not only occurred around the apex but extended a few millimetres coronally, along the root surface. Lee & Messer (1986) suggested that the detection of an artificially created lesion should be easier than those occurring naturally, because of the marked variation in density at the outer border of the cavity, relative to the normal trabecular pattern. Indeed, in this study, when a lesion was present, it was clearly visualized whether the arc of rotation was 360° or 180°.

Only when the two scans (180° and 360°) were viewed together, could some slight 'streaking', and loss of image quality, be perceived in the 180° scan that was not as prominent in the 360° scans; however, this did not diminish the diagnostic yield of the image produced. Diagnostic difficulties were encountered however, when analysing the samples with pre-existing, sparse trabecular patterns. The area under investigation was already highly radiolucent, making the discrimination of a small, subtle change in the relative density even more challenging. This was reflected in the results, which revealed a broad range of specificity for both scan parameters (0.57–0.92). None of the readers scored perfectly in terms of specificity. Furthermore, wide variation was seen for intra-examiner scores ranging from 26 to 100%; this will be discussed further in a later section. Vandeberghe *et al.* (2008) suggest that the detail of trabecular pattern was better visualized by intra-oral digital images, which had superior resolution.Finally, the examiners in this study were presented with the full data set, which increased the volume of data to interpret. This methodology differs from many other CBCT studies, which presented their readers with the static images in three planes (Stavropoulos & Wenzel 2007, Ozen *et al.* 2009).

Receiver operating characteristic analyses provide additional information on the diagnostic accuracy of a test (Metz 1978, Swets 1979). The ROC curve is a plot of sensitivity (y-axis) against false positive rates (1-specificity) on the x-axis. It includes all the cut-off points, rather than the binary cut-off (present/absent) generated when calculating sensitivity or specificity values (Obuchowski 2003). In this study, the cut-off points were along the five-point confidence scale, alluded to earlier. As it is determined using sensitivity and specificity data, the ROC is also independent of disease prevalence. The advantage of ROC analyses over sensitivity or specificity values is that it allows direct comparison between two tests using a common set of scales, at all possible cut-off points (Metz 2006). It allows diagnostic accuracy to be expressed as single figure, which is particularly useful when comparison between two diagnostic methods is being made. As with sensitivity and specificity calculation, the closer the area under the ROC curve is to 1.0, the better the diagnostic test is. As a test measure, ROC is also independent of the prevalence of disease. The findings in this study for mean ROC values were 0.852 and 0.872 for the 360° and 180° scans, respectively. This was considerably lower than the findings in a recent study with a similar methodology (Patel *et al.* 2009c). Their study demonstrated an average ROC value of 1.0, for both small and large artificially created lesions, in (dry) human mandibles. Metz (2006) cites reader and/or case sample variation as an explanation for the inability to replicate experimental results under different conditions.

The positive or negative predictive value of a test is another method by which its diagnostic accuracy can be described. The PPV of a test are defined as the proportion of patients with a positive test results correctly diagnosed as such (Altman & Bland 1994). It differs subtly to sensitivity, in that it is dependent on the prevalence of the disease.

Overall, the PPV were 89.1% and 93.2% for the 360° and the 180° scans, respectively. These values compare favourably with those of de Paula-Silva *et al.* (2009), which demonstrate PPV and NPV for CBCT of 100% and 46%, respectively. The NPV calculated in this study were 76% and 74.3% again for the 360° and the 180° scans, respectively.

The findings of this current study revealed a wide range in interobserver variability from 26% to 100% in the 360° scans. The range for 180° was not so broad, 33–100%. When these results were narrowed to assess only the most experienced examiners, the range was reduced by 13% for the 360° scans (39–100%) and by 15% for the 180° scans (48–100%). The overall mean scores were classified as moderate for the 360° scans and substantial for the 180° scans, in each session or in a single session. Sogur *et al.* (2007) found intra-examiner agreement with the Accuitomo 3D ranged from 0.162 to 0.772 when evaluating root canal filled teeth. In an evaluation of chemically created artificial lesions, Ozen *et al.* (2009) revealed inter- and intra-observer values ranging from 0.417 to 0.461 and 0.533 to 0.699 for CBCT. The overall combined (360° & 180°) mean interobserver value in this study was 0.603, compared with 0.722 in a recent study with a similar methodology (Patel 2009, Patel *et al.* 2009c). Patel *et al.* (2009a) also produced a higher mean intra-observer kappa score of 0.64, compared with the findings of this study 0.232. This may be explained by the presentation of the data, which was different in these studies. Patel *et al.* (2009a) presented static images, whereas the current study presented the examiners with the full data set, in keeping with the normal presentation of CBCT data in a clinical setting. It was expected that having access to the full data set would ameliorate the diagnostic accuracy. However, it appears that by having a larger volume of data to interpret, it may have compromised the reproducibility, as reflected by 'fair' intra-examiner reproducibility.

High accuracy demonstrated by an ROC value approaching 1.0, may imply high agreement, determined by Cohen kappa statistics. However, high agreement does not necessarily imply high accuracy (Kundel & Polansky 2003). It is accepted that interexaminer reproducibility is subject to wide variation. This may be due in part to the complexity of the decision-making process. Reit & Hollender (1983) found only 39% agreement between examiners. This study used six experienced examiners. They suggested that the greatest diagnostic difficulty was encountered when the more subtle signs of periapical inflammatory changes were assessed (i.e. widened periodontal ligament space or small periapical lesions). Reit (1987) suggested that observer calibration may be of limited value in reducing the incidence of observer disagreement. The complexities of the decision-making process (scientific, psychological and sociological) are cited as contributory. On the other hand, in a long-term follow-up study, Molven *et al.* (2002) found 83% overall agreement between two experienced observers. They found that joint evaluation might play a role in reducing observer variation.

A human cadaver model investigating naturally occurring lesions of endodontic origin may overcome some of the limitations presented by the present *ex vivo* study design. The naturally occurring apical lesions would be more representative of the clinical situation. However, the number of specimens required to provide sufficient numbers of teeth with associated periapical changes could be vast and beyond the remit of a study such as this. Chemically created lesions, for example using 70% perchloracetic acid, have been proposed as an alternative to the traditional *ex vivo* model where apical lesions are simulated with a bur (Ozen *et al.*

2009). The authors suggested that the chemically created lesion better replicates the characteristics of naturally occurring lesions of endodontic origin. This was represented by diffuse borders and an advancing front of demineralization, characteristic of *in vivo* situation. However, the standardization of the size of a chemically induced lesion is open to question.

In the clinical situation, the X-ray beam is attenuated and scatter occurs when the photons hit the soft tissues prior to penetrating the object. To replicate this situation in an *ex vivo* model, first, the mandibles were rehydrated in keeping with previous study methodology (Patel *et al.* 2009a). An acrylic cylinder was placed over the mandibles to attenuate the beam in a similar fashion, to the presence of the oral soft tissues (Noujeim *et al.* 2009). Pilot work confirmed that the images produced were comparable to similar clinical samples.

Every effort was made to optimize the viewing conditions. The radiographic assessments were carried out in a quiet, dimly lit room (Welander *et al.* 1983). Other factors were also considered, such as appropriate position of lighting (ideally overhead, but out of field of view) and reflections from the screen were minimized (i.e. no open doorways or windows directly behind the operator). The utility to calibrate the monitors to DICOM Part 14 compliance was carried out using RadicCS V3.22, to optimize the quality control of the images being viewed (Samei *et al.* 2005).

In conclusion, it is also worth mentioning that CBCT users could also benefit from alternative optimization strategies, considering that a partial rotation option is not available on all CBCT machines. Similarly to a reduced arc of rotation, reduction in exposure factors and hence dose could be achieved through a different range of settings of kV and mA. Reducing the mA, whilst maintaining a full 360° rotation, might be a good option, whereas tuning down the kV might prove less predictable in the reduction in the effective dose (Tsiklakis *et al.* 2005).

Conclusion

Both 360° and 180° cone-beam computed tomography scans yield similar accuracy in the detection of periapical bone loss. Further studies may analyse the effective reduction in the dosimetric exposure for the patients, which may represent a substantial advantage of a reduced scanning arc as required by the ICRP guidance of as low as reasonably achievable.

References

Altman DG, Bland JM (1994) Diagnostic tests 2: predictive values. *British Medical Journal (Clinical Research Ed.)* **309**, 102.

Arai Y, Tammisalo E, Iwai K, Hashimoto K, Shinoda K (1999) Development of a compact computed tomographic apparatus for dental use. *Dentomaxillofacial Radiology* **28**, 245–8.

Bender IB, Seltzer S (1961a) Roentgenographic and direct observation of experimental lesions in bone: I. *Journal of the American Dental Association* **62**, 152–60.

Bender IB, Seltzer S (1961b) Roentgenographic and direct observation of experimental lesions in bone: II. *Journal of the American Dental Association* **62**, 708–16.

Brown AA, Scarfe WC, Scheetz JP, Silveira AM, Farman AG (2009) Linear accuracy of cone beam CT derived 3D images. *Angle Orthodontics* **79**, 150–7.

Dummer PM, Hicks R, Huws D (1980) Clinical signs and symptoms in pulp disease. *International Endodontic Journal* **13**, 27–35.

Durack C, Patel S, Davies J, Wilson R, Mannocci F (2011) Diagnostic accuracy of small volume cone beam computed tomography and intraoral periapical radiography for the detection of simulated external inflammatory root resorption. *International Endodontic Journal* **44**, 136–47.

ESE (2006) Quality guidelines for endodontic treatment: consensus report of the European Society of Endodontology. *International Endodontic Journal* **39**, 921–30.

Estrela C, Bueno MR, Leles CR, Azevedo B, Azevedo JR (2008) Accuracy of cone beam computed tomography and panoramic and periapical radiography for detection of apical periodontitis. *Journal of Endodontics* **34**, 273–9.

Faccioli N, Barillari M, Guariglia S *et al.* (2009) Radiation dose saving through the use of cone-beam CT in hearing-impaired patients. *Radiology Medicine* **114**, 1308–18.

Garcia de Paula-Silva FW, Hassan B, Bezerra da Silva LA, Leonardo MR, Wu MK (2009) Outcome of root canal treatment in dogs determined by periapical radiography and cone-beam computed tomography scans. *Journal of Endodontics* **35**, 723–6.

Goldman M, Pearson A, Darzenta N (1972) Endodontic success, who's reading the radiograph? *Oral Surgery, Oral Medicine, Oral Pathology* **33**, 432–7.

Horner K, Islam M, Flygare L, Tsiklakis K, Whaites E (2009) Basic principles for use of dental cone beam computed tomography: consensus guidelines of the European Academy of Dental and Maxillofacial Radiology. *Dentomaxillofacial Radiology* **38**, 187–95.

Huumonen S, Ørstavik D (2002) Radiological aspects of apical periodontitis. *Endodontic Topics* **1**, 3–25.

Jonasson G, Alstad T, Vahedi F, Bosaeus I, Lissner L, Hakeberg M (2009) Trabecular pattern in the mandible as bone fracture predictor. *Oral Surgery, Oral Medicine, Oral Pathology, Oral Radiology and Endodontics* **108**, 42–51.

Jorge EG, Tanomaru-Filho M, Goncalves M, Tanomaru JMG (2008) Detection of periapical lesion development by conventional radiography or computed tomography. *Oral Surgery, Oral Medicine, Oral Pathology, Oral Radiology and Endodontics* **106**, 56–61.

Kundel HL, Polansky M (2003) Measurement of observer agreement. *Radiology* **228**, 303–8.

Lee SJ, Messer HH (1986) Radiographic appearance of artificially prepared periapical lesions confined to cancellous bone. *International Endodontic Journal* **19**, 64–72.

Lofthag-Hansen S, Huumonen S, Grondahl K, Grondahl H-G (2007) Limited cone-beam CT and intraoral radiography for the diagnosis of periapical pathology. *Oral Surgery, Oral Medicine, Oral Pathology, Oral Radiology and Endodontics* **103**, 114–9.

Ludlow JB, Ivanovic M (2008) Comparative dosimetry of dental CBCT devices and 64-slice CT for oral and maxillofacial radiology. *Oral Surgery, Oral Medicine, Oral Pathology, Oral Radiology and Endodontics* **106**, 106–14.

Metz CE (1978) Basic principles of ROC analysis. *Seminars in Nuclear Medicine* **8**, 283–98.

Metz C (2006) Receiver operating characteristic analysis: a tool for the quantitative evaluation of observer performance and imaging systems. *Journal of the American College of Radiology* **3**, 413–22.

Molven O, Halse A, Fristad I (2002) Long-term reliability and observer comparisons in the radiographic diagnosis of periapical disease. *International Endodontic Journal* **35**, 142–7.

Ng YL, Mann V, Gulabivala K (2008a) Outcome of secondary root canal treatment: a systematic review of the literature. *International Endodontic Journal* **41**, 1026–46.

Ng YL, Mann V, Rahbaran S, Lewsey J, Gulabivala K (2008b) Outcome of primary root canal treatment: systematic review of the literature – Part 2. Influence of clinical factors. *International Endodontic Journal* **41**, 6–31.

Noujeim M, Prihoda T, Langlais R, Nummikoski P (2009) Evaluation of high-resolution cone beam computed tomography in the detection of simulated interradicular bone lesions. *Dentomaxillofacial Radiology* **38**, 156–62.

Obuchowski NA (2003) Receiver operating characteristic curves and their use in radiology. *Radiology* **229**, 3–8.

Ozen T, Kamburoglu K, Cebeci AR, Yuksel SP, Paksoy CS (2009) Interpretation of chemically created periapical lesions using 2 different dental cone-beam computerized tomography units, an intraoral digital sensor, and conventional film. *Oral Surgery, Oral Medicine, Oral Pathology, Oral Radiology and Endodontics* **107**, 426–32.

Patel S (2009) New dimensions in endodontic imaging: part 2. Cone beam computed tomography. *International Endodontic Journal* **42**, 463–75.

Patel S, Horner K (2009) The use of cone beam computed tomography in endodontics. *International Endodontic Journal* **42**, 755–6.

Patel S, Dawood A, Mannocci F, Wilson R, Pitt Ford T (2009a) Detection of periapical bone defects in human jaws using cone beam computed tomography and intraoral radiography. *International Endodontic Journal* **42**, 507–15.

Patel S, Dawood A, Whaites E, Pitt Ford T (2009b) New dimensions in endodontic imaging: part 1. Conventional and alternative radiographic systems. *International Endodontic Journal* **42**, 447–62.

Patel S, Dawood A, Wilson R, Horner K, Mannocci F (2009c) The detection and management of root resorption lesions using intraoral radiography and cone beam computed tomography - an *in vivo* investigation. *International Endodontic Journal* **42**, 831–8.

de Paula-Silva FW, Wu MK, Leonardo MR, da Silva LA, Wesselink PR (2009) Accuracy of periapical radiography and cone-beam computed tomography scans in diagnosing apical periodontitis using histopathological findings as a gold standard. *Journal of Endodontics* **35**, 1009–12.

Pitt Ford TR (1984) The radiographic detection of periapical lesions in dogs. *Oral Surgery Oral Medicine Oral Patholology* **57**, 662–7.

Pitt Ford T, Patel S (2004) Technical equipment for assessment of dental pulp status. *Endodontic Topics* **7**, 2–13.

Ramadan A, Mitchell D (1962) A roentgenographic study of experimental bone destruction. *Oral Surgery, Oral Medicine, Oral Pathology* **15**, 934–43.

Razavi T, Palmer RM, Davies J, Wilson R, Palmer PJ (2010) Accuracy of measuring the cortical bone thickness adjacent to dental implants using cone beam computed tomography. *Clinical Oral Implants Research* **21**, 718–25.

Reit G (1987) Decision strategies in endodontics: on the design of a recall program. *Dental Traumatology* **3**, 233–9.

Reit C, Hollender L (1983) Radiographic evaluation of endodontic therapy and the influence of observer variation. *Scandinavian Journal of Dental Research* **91**, 205–12.

Samei E, Badano A, Chakraborty D *et al.* (2005) Assessment of display performance for medical imaging systems: executive summary of AAPM TG18 report. *Medical Physics* **32**, 1205–25.

Scarfe WC, Farman AG (2008) What is cone-beam CT and how does it work? *Dental Clinics of North America* **52**, 707–30.

Schwartz S, Foster J (1971) Roentgenographic interpretation of experimentally produced bony lesions. *Oral Surgery, Oral Medicine, Oral Pathology* **32**, 606–12.

Seltzer S, Bender L, Ziontz M (1963) The dynamics of pulp inflammation: correlation between diagnostic data and actual histologic findings in the pulp. *Oral Surgery, Oral Medicine and Oral Pathology* **16**, 846–71.

Sogur E, Baksi BG, Gröndahl HG, Lomcali G, Sen BH (2009) Detectability of chemically induced periapical lesions by limited cone beam computed tomography, intra-oral digital and conventional film radiography. *Dentomaxillofacial Radiology* **38**, 458–64.

Stavropoulos A, Wenzel A (2007) Accuracy of cone beam dental CT, intraoral digital and conventional film radiography for the detection of periapical lesions. An ex vivo study in pig jaws. *Clinical Oral Investigations* **11**, 101–6.

van der Stelt PF (1985) Experimentally produced bone lesions. *Oral Surgery, Oral Medicine, Oral Pathology* **59**, 306–12.

Swets JA (1979) ROC analysis applied to the evaluation of medical imaging techniques. *Investigative Radiology* **14**, 109–21.

Tsiklakis K, Donta C, Gavala S, Karayianni K, Kamenopoulou V, Hourdakis CJ (2005) Dose reduction in maxillofacial imaging using low dose Cone Beam CT. *European Journal of Radiology* **56**, 413–7.

Vandenberghe B, Jacobs R, Yang J (2008) Detection of periodontal bone loss using digital intraoral and cone beam computed tomography images: an *in vitro* assessment of bony and/or infrabony defects. *Dentomaxillofacial Radiology* **37**, 252–60.

Welander U, McDavid WD, Higgins NM, Morris CR (1983) The effect of viewing conditions on the perceptibility of radiographic details. *Oral Surgery, Oral Medicine, Oral Pathology* **56**, 651–4.

Wengraf A (1964) Radiologically occult bone cavities. *British Dental Journal* **117**, 532.

Whaites E (2007) *Essentials of Dental Radiology and Radiography*, 4th edn. Philadelphia, PA, USA: Churchill Livingston Elsevier.